231908

UCRL-JC-124445 Rev 1
PREPRINT

Absolute Equation of State Measurements of Shocked Liquid Deuterium up to 200 GPa (2 Mbar)

K. S. Budil, L. B. Da Silva, P. Celliers, G. W. Collins, N. C. Holmes,
T. W. Barbee Jr., B. A. Hammel, J. D. Kilkenny, R. J. Wallace,
M. Ross, G. Chiu, A. Ng, R. Cauble

This paper was prepared for submittal to the
6th International Workshop on the Physics of Compressible Turbulent Mixing
Marseille, France
June 18-21, 1997

June 10, 1997

Lawrence Livermore National Laboratory

Absolute Equation of State Measurements of Shocked Liquid Deuterium up to 200 GPa (2 Mbar)

K. S. Budil[1], L. B. Da Silva[1], P. Celliers[1], G. W. Collins[1], N. C. Holmes[1], T. W. Barbee Jr. [1], B. A. Hammel[1], J. D. Kilkenny[1], R. J. Wallace[1], M. Ross[1], G. Chiu[2], A. Ng[2], and R. Cauble[1]
[1]Lawrence Livermore National Laboratory
P. O. Box 808, L-473, Livermore, CA 94550 USA
[2]University of British Columbia, Vancouver, B. C., Canada

Abstract: We present results of the first measurements of density, shock speed and particle speed in compressed liquid deuterium at pressures in excess of 1 Mbar. We have performed equation of state (EOS) measurements on the principal Hugoniot of liquid deuterium from 0.2 to 2 Mbar. We employ high-resolution radiography to simultaneously measure the shock and particle speeds in the deuterium, as well as to directly measure the compression of the sample. We are also attempting to measure the color temperature of the shocked D_2. Key to this effort is the development and implementation of interferometric methods in order to carefully characterize the profile and steadiness of the shock and the level of preheat in the samples. These experiments allow us to differentiate between the accepted EOS model for D_2 and a new model which includes the effects of molecular dissociation on the EOS.

1. Introduction

Experimentally verified equations of state do not exist for many materials in the multi-Mbar regime due to the inherent difficulties of achieving such high pressures. While high intensity lasers can readily produce shocks in this pressure regime, the requirements for an accurate EOS measurement present formidable difficulties for laser experiments. Thus, there have been few laser-driven EOS experiments despite the fact that the EOS is crucial for hydrodynamic descriptions of laser experiments. Accuracy sufficient to differentiate between various EOS models is difficult to obtain for many reasons. The initial condition of the sample may be difficult to determine due to preheat, the shock may not be spatially uniform and planar or its velocity may not be steady in time.

The EOS of hydrogen and its isotopes at high pressure are extremely important to the physics of high density matter.1, 2 The EOS in the 1-10 Mbar regime largely determines the internal structure of Jovian planets.3 In inertial confinement fusion (ICF), the performance of deuterated capsules is critically dependent upon shock timing and efficient compression which in turn rely on the EOS.4 While several theoretical models of the EOS of hydrogen have been proposed, 5, 6, 7, 8 outstanding questions still exist, for instance the transition from a diatomic to a monatomic fluid. Previous experiments have obtained data for hydrogen at pressures greater than 100 GPa by both dynamic shock compression and static compression in diamond anvil cells.9 The temperatures and densities achievable via shock compression are directly applicable to ICF and the most accurate data were produced using light gas guns.10, 11

While early impedence match measurements of the EOS of H_2 and D_2 were found to be

[0]More information - Email: budil1@llnl.gov

in good agreement with a model which neglected dissociation,10 recent experiments revealed significantly lower temperatures than predicted for pressures higher than 20 GPa.11 A new model that incorporates the effect of dissociation of the molecular fluid was formulated. 11 It is based on the ideal mixing of molecular and monatomic metallic hydrogen states and includes a single adjustable parameter. This model predicts that deuterium is significantly more compressible in the 20-1000 GPa regime, predicting 50% density that calculated from the previous model and the D_2 table in the widely-used Sesame EOS library.12

2. Experimental design

2.1. Shock compression of materials

Shock compression utilizeing a single shock drives a fluid to a point on the principal Hugoniot. The Hugoniot is the locus of all final states of pressure, energy and density that can be achieved behind a single shock wave passing through a material from an initial state. The shock speed U_s, particle speed U_p, the pressure P, and final density ρ are related by

$$P - P_o = \rho_o U_s U_p \tag{1}$$

and

$$\rho/\rho_o = U_s/(U_s - U_p), \tag{2}$$

where ρ_o is the initial denstiy, P_o is the initial pressure and ρ/ρ_o is the compression.13 These relations require that two independent parameters be measured to obtain an absolute data point.

In these experiments, liquid deuterium was compressed by a laser-driven shock wave launched from an aluminum pusher. High resolution streaked radiographs of the aluminum-D_2 interface were obtained which allow direct measurement of the shock speed in the deuterium, the particle speed (Al pusher speed), and compression, which yields the density provided the initial density is well-known.

2.2. Experimental configuration

The experimental configuration is illustrated in Figure 2.2.. Figure 2.2.a shows the cryogenic

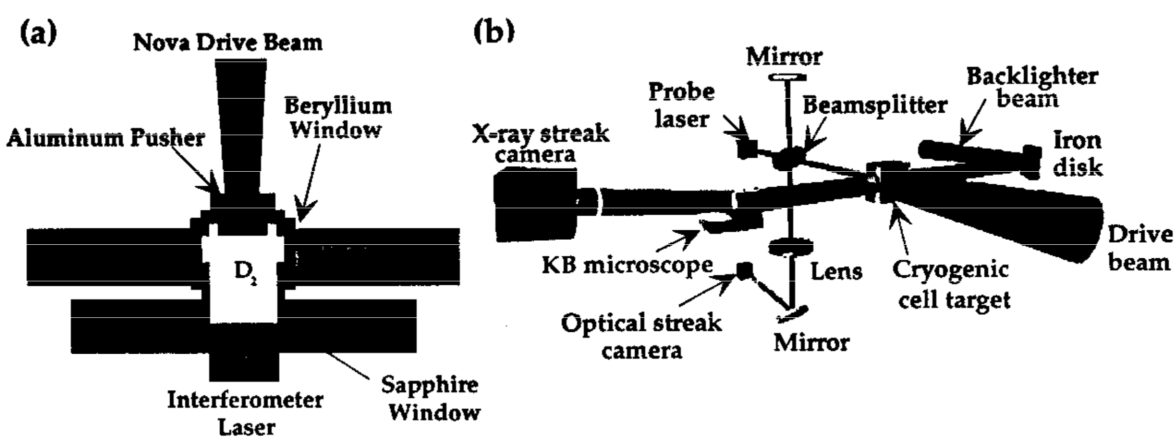

Figure 1. (a) Diagram of the cryogenic cell used in the experiment. (b) Experimental layout for the deuterium EOS measurement.

cell used to contain the liquid D_2. The cell was a cylinder 450 μm long by 1 mm in diameter machined into a solid copper block. A solid aluminum pusher sealed one end of the cell. Pusher thicknesses of 100, 180 and 250 μm were used for various experiments. The side of the aluminum external to the cell was coated with 15 to 25 μm of polystyrene and a 100 nm layer of aluminum. The Al overcoat prevents direct laser shine through the plastic and the polystyrene ablator prevented direct laser ablation of the Al pusher. The low Z material minimizes x-ray emission and consequent preheating of the pusher from x rays produced in the ablator plasma. A 500 μm diameter window was drilled into each side of the cell and sealed with a 5 μm thick beryllium foil to allow the backlighter x rays to transmit through the cell.

The cell was loaded with liquid D_2 (99.98% pure containing 33% J=1 molecules) at 19.4-19.8 K (monitored to within 0.05 K) and then pressurized to a few hundred Torr. The D_2 density was determined from the saturation curve16 and was typically 0.171 g/cm^3. The initial density ρ_o was known for each experiment with an uncertainty of less that 0.1%.

The targets were directly-driven by one beam of the Nova laser at $\lambda = 527$ μm as illustrated in Figure 2.2.b. The laser beam irradiance profile was smoothed with a kinoform phase plate and focused onto the target in an elliptical spot with major and minor diameters of up to 900 and 600 μm respectively, depending upon the focusing. The laser pulse was 8 or 10 ns square and produced intensities in the range of 5×10^{12} to 2×10^{14} W/cm^2. A second Nova beam was focused onto an iron foil (10 ns at 6×10^{13} W/cm^2) to generate 800 eV x rays to radiograph the sample. The backlighter was placed 12 cm away from the target cell to eliminate heating of the cell and to produce a near-collimated x-ray source. The transmitted x rays were imaged by a Kirkpatrick-Baez (K-B) microscope onto a streak camera. The K-B used two tungsten/rhenium-coated 6-m-radius of curvature spherical mirrors which provided a bandpass of 750-840 eV with a 2.5 mrad collection half-angle. The resolution of the K-B microscope was found to be better than 3 μm over a 300 μm field of view and it was used at magnifications of 33$\times$ and 82$\times$. A strip 300 μm long by 5 to 30 μm wide was imaged depending upon the magnification.

2.3. Target characterization

Since the accuracy of the measurement is critically dependent upon the initial conditions of the experiment, some effort was expended to characterize the shock planarity and steadiness as well as the level of preheating experienced by the deuterium. Figure 2.3. shows interferograms obtained with a 100 μm thick pusher overcoated with a 20 μm thick polystyrene ablator irradiated at two intensities. When the target was at $\sim 8.5 \times 10^{13}$W/cm^2, motion of the aluminum-deuterium interface is clearly observed beginning approximately 2 ns prior to shock breakout as shown in Figure 2.3.a. A simple thermal expansion model estimates the temperature at this surface to be $\sim$ 1000 K. When the intensity was reduced to $\sim 1.5 \times 10^{13}$W/cm^2, as shown in Figure 2.3.b, no evidence of preheating (T < 400 K) is observed. The secondary curvature of the shock front is due to the "tophat", or reentrant, design of the pusher. Aluminum plasma from the sides of the tophat moves into the path of the drive beam during its 8 ns duration, effectively reducing the drive laser intensity at the outer perimeter of the aluminum, slowing down the shock considerably at the edges of the target. The shock in either case is observed to be planar and uniform to within $\pm$ 2.5 μm over the central 350 μm of the target, quite adequate for these measurements.

Figure 2. (a) Interferogram obtained from a target irradiated at $\sim 8.5\times10^{13}\mathrm{W/cm^2}$. (b) Interferogram obtained from a target irradiated at $\sim 1.5\times10^{13}\mathrm{W/cm^2}$.

3. Experimental results

Once the issue of preheat and shock planarity had been addressed, streaked radiography of the deuterium-filled cells was utilized to measure the shock speed, particle speed, and compression of the material. A representative radiograph is shown in Figure 3. Here a drive irradiance of

Figure 3. Streaked radiograph of the aluminum-deuterium interface used to determine the shock and particle speeds and the compression of the deuterium.

10^{14} W/cm^2 over 8 ns was used. Bright regions of the image correspond to high transmission of the backlighter x rays. At 2 ns the laser-driven shock wave crosses the aluminum-deuterium interface and the pusher begins to move at a steady speed, the particle speed. The shock front can be seen moving through the deuterium as a dark line in the image produced by backlighter x rays being refracted by the jump in density between the shocked and unshocked deuterium, similar to the Schlieren technique for detecting density gradients. Shock reverberations in the pusher cause a second shock to be launched into the D_2 at approximately 6 ns, and the propogation of the shock front and interface are both steady until its arrival. Only data from the steady-propagation region were used in the EOS calculations.

The measured shock speeds and final densities are shown in Figure 3.a. The open squares

Figure 4. (a) Shock speed versus density. (b) Pressure versus density. In both plots, open diamonds represent gas gun data from Nellis *et al.* and open squares with error bars are from this measurement.

with error bars are from this measurement and the accuracy with which the slopes of the shock and interface trajectories can be measured largely determines the error bars on the data. Hugoniots calculated using the Sesame EOS table[14] and the new dissociation model[11] are shown along with data obtained from previous gas gun experiments[10]. Our data are in good agreement with the gas gun results at low compression while the higher compression data deviate significantly from the Sesame prediction. The data support the higher compression predicted by the dissociation model and we therefore conclude that molecular dissociation is indeed significant in hydrogen isotopes at compressions near 100 Gpa. Figure 3.b shows pressure versus density for these measurements.

4. Conclusion

We have presented the first measurement of density, shock and particle speeds in liquid deuterium at pressures ranging from 25 to 210 Gpa. Interferometric characterization of the shock and aluminum pusher showed that the laser-driven shock wave was planar and that there was no significant preheating of the deuterium. High-resolution, time-resolved radiographs confirm that the shock is steady in time and allow for determination of absolute Hugoniot data. These data strongly indicate that a dissociative transition from a diatomic to a monatomic fluid state occurs in the deuterium and provide support for a revised equation of state model in this pressure regime.

Acknowledgement. The authors would like to thank S. Dixit for the kinoform phase plate, D. A. Young, F. J. Rogers and R. M. More for useful discussions on the theory, S. G. Glendinning for help with image processing, T. Weiland for assistance with the interferometer laser, W. Unites, R. Jones, J. Burman, S. Letts, E. Mapoles, J. Pipes, and J. Sanchez for assembly of the cryostat and cells, J. Cox, and K. Haney for diagnostic development, J. Cardinal and D. Cocherell for diagnostic design and installation, the Nova target fabrication group, and the Nova operations technical support personnel.

A. N. and G. C. acknowledge the support of the Natural Sciences and Engineering Research Council of Canada. This work was performed by the Lawrence Livermore National Laboratory under the auspices of the U. S. Department of Energy under Contract No. W-7405-ENG-48.

References

[1] Ichimaru S, Iyetomi H and Tanaka S
Phys. Rep.,149, 91, (1987).

[2] Ashcroft N W
Phys. World, 8, 43, (1995).

[3] Smoluchowski R
Nature, 215, 691, (1967). Zharkov V N and Trubitsyn V P
in *Jupiter*, T. Gehrels, Ed., (Univ. of Arizona press, Tucson, 1976), 135-175. Hubbard W B, Science, 214, 145, (1981). Stevenson D J,
Annu. Rev. Earth Planet Sci., 10, 257, (1982). Nellis W J, Ross M, and Holmes N C,
Science, 269, 1249, (1995).

[4] Lindl J,
Phys. Plasmas, 2, 3933, (1995).

[5] Hubbard W B,
Astrophys. J., 152, 745, (1968).

[6] Ross M, Ree F H, Young D A,
J. Chem. Phys., 79, 1487, (1983).

[7] Saumon D, Chabrier G, and Van Horn H M,
Astrophys. J. Supp., 99, 713, (1995).

[8] Magro W R, Ceperley D M, Pierleoni C, and Bernu B
Phys. Rev. Lett., 76, 1240, (1996).

[9] Mao H K and Hemley R J Rev. Mod. Phys., 66, 671, (1994).

[10] Nellis W J, Mitchell A C, van Theil M, Devine G J, Trainor R J, and Brown N,
J. Chem. Phys., 79, 1480, (1983).

[11] Holmes N C, Ross M, and Nellis W J,
Phys. Rev. B, 52, 15835, (1995).

[12] Weir S T, Mitchell A C, and Nellis W J,
Phys. Rev. Lett., 76, 1860, (1996).

[13] Zel'dovich Y B and Raizer Y P, *Physics of Shock Waves and High-Temperature Hydrodynamic Phenomena*, (Academic Press, New York, 1966).

[14] Kerley G I,
Los Alamos Scientific Laboratory Report LA-4776, January, (1972).

[15] van Kessel C G M and Sigel R,
Phys. Rev. Lett., 33, 1020, (1974). Tanaka K A *et al.*,
in *Shock Waves*, ed. K. Takayama (Springer-Verlag, Berlin, 1992), p. 863.

[16] Souers P C, *Hydrogen Properties for Fusion Energy*, (University of California Press, Berkeley, 1986). Budil K S *et al.* "Characterization of preheat in laser-driven targets using interferometry", presented at the *38th Meeting of the Division of Plasma Physics of the American Physical Society*, Denver, Colorado, November 1996.

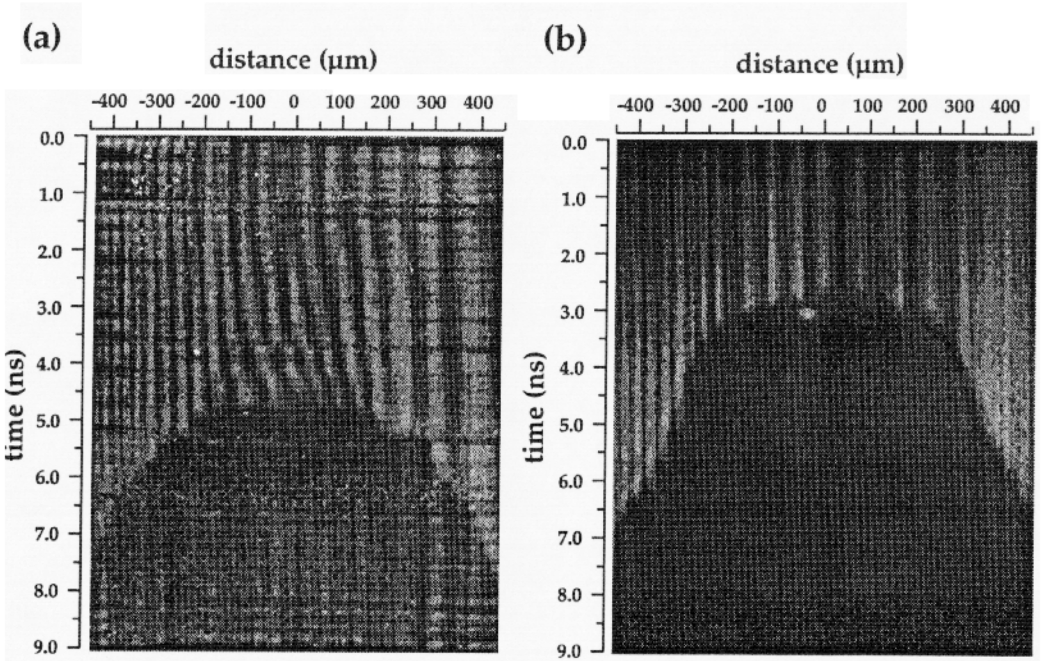
(a)
distance (μm)
-400 -300 -200 -100 0 100 200 300 400
time (ns)
0.0 1.0 2.0 3.0 4.0 5.0 6.0 7.0 8.0 9.0
(b)
distance (μm)
-400 -300 -200 -100 0 100 200 300 400
time (ns)
0.0 1.0 2.0 3.0 4.0 5.0 6.0 7.0 8.0 9.0

Fig. 4

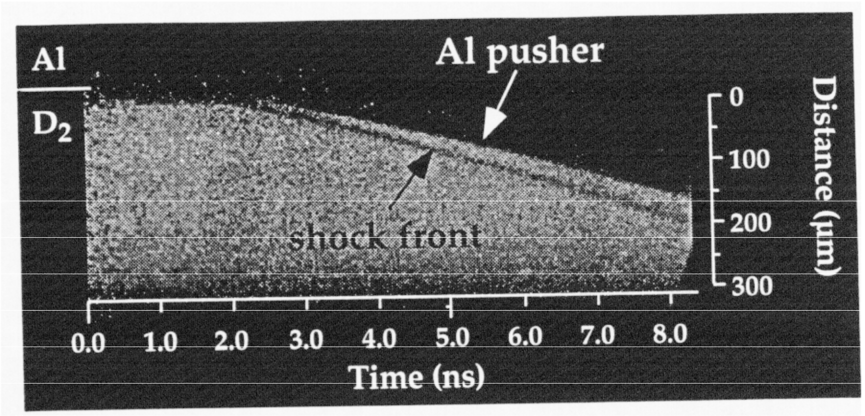
Al
D2
Al pusher
shock front
0
100
200
300
Distance (μm)
0.0
1.0
2.0
3.0
4.0
5.0
6.0
7.0
8.0
Time (ns)

Fig. 3

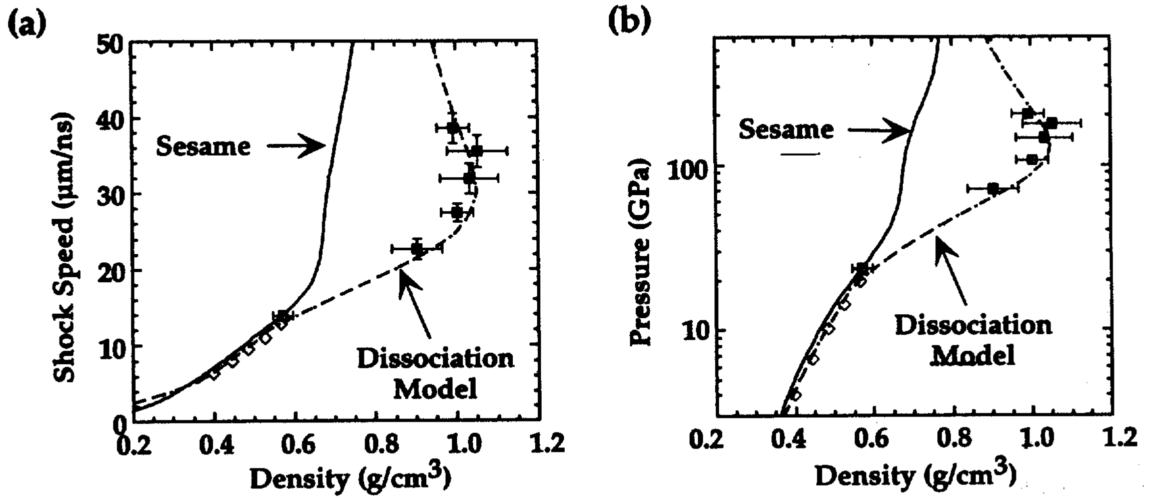
(a)
Shock Speed (μm/ns)
Sesame
Dissociation
Model
Density (g/cm3)
(b)
Pressure (GPa)
Sesame
Dissociation
Model
Density (g/cm3)

Fig. 4

Technical Information Department • **Lawrence Livermore National Laboratory**
University of California • Livermore, California 94551